Neighboring Group Effects on the Rates of Cleavage of Si–O–Si-Containing Compounds

Ethan A. Gormong, Dorian S. Sneddon, Theresa M. Reineke,* Thomas R. Hoye*

Department of Chemistry, University of Minnesota, 207 Pleasant St., SE, Minneapolis, Minnesota 55455

TOC GRAPHIC

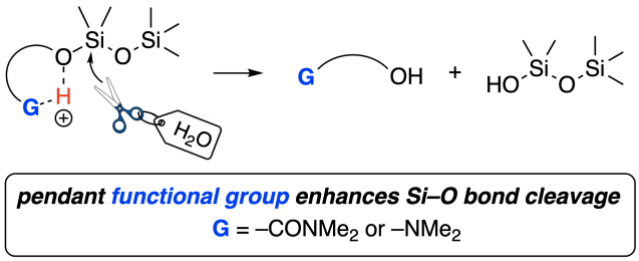

ABSTRACT

The presence of a nearby tethered functional group (G, G = tertiary amide or amine) can significantly impact the rate of cleavage of an Si–O bond. We report here an *in situ* ^{1}H NMR spectroscopic investigation of the relative rates of cleavage of model substrates containing two different Si–O substructures, namely alkoxydisiloxanes [GRO–Si(Me_2)–O–$SiMe_3$] and carbodisiloxanes [GR–Si(Me_2)–O–$SiMe_3$]. The trends in the relative rates (which slowed with increasing chain length, with a notable exception) of alkoxydisiloxane hydrolyses were probed via computation. The results correlated well with the experimental data. In contrast to the hydrolysis of the alkoxydisiloxanes, the carbodisiloxanes were not fully hydrolyzed, but rather formed equilibrium mixture of starting asymmetric disiloxane, two silanols, and a new symmetrical disiloxane. We also uncovered a facile siloxy-metathesis reaction of an incoming silanol with the carbodisiloxane substrate [e.g., Me_2NR–Si(Me_2)–O–$SiMe_3$ + $HOSiEt_3$ ⇋ Me_2NR–Si(Me_2)–O–$SiEt_3$ + $HOSiMe_3$] facilitated by the pendant dimethylamino group, a process that was also probed by computation.

INTRODUCTION

Compounds containing silicon-oxygen bonds are widely encountered in organic, polymer, and materials chemistries. The specific substructural environment of an Si–O bond significantly influences its kinetic and thermodynamic properties. In turn, this determines the suitability of the specific functional group [R_3SiOR', $R_2Si(OR')_2$, $RSi(OR')_3$, $Si(OR')_4$]; R' = C and/or Si] for myriad applications (e.g., protecting group chemistry, silicone polymers, surface modifications, sealants, sol-gels). The lability of the Si–O-containing moiety influences the utility of these siloxy compounds by impacting features such as cure rates,[1] dynamics of covalent adaptable network reorganization,[2] release-rates,[3] and post-use degradation in the environment.[4]

While it has long been known that decreasing the steric bulk around the silicon atom elevates the rate of Si–O cleavage via nucleophilic attack,[5] the participation of an appropriate tethered neighboring functional group can also increase the rate of cleavage of Si–O bonds. Researchers at Bayer AG observed hydrolysis rate enhancement in the early 1960s when studying pre-polymers bearing labile alkoxysilane endgroups.[6] Those featuring amino ($–NR_2$), carboalkoxy (–OC(O)R), or carbamoyl (–N(H)COOMe) functional groups near the silicon underwent rapid hydrolysis. This phenomenon was explored in much greater detail in a small-molecule study of alkoxysilanes by Tacke and coworkers in 2014,[7] with an additional follow-up report in 2016 (Figure 1a).[8] These authors reported the relative rates of hydrolysis of a wide range of substrates (measured by ^{1}H NMR spectroscopy), varying the length of the tether between G and Si, the nature of the alkyl substituents on Si, and the bulk of the alkoxy leaving group at pH ≈ 5 and 11. Compounds featuring α-, β-, and γ- amino or carbamate groups displayed rapid hydrolysis under acidic conditions. The authors rationalized these observations

by proposing hydrogen bond-assisted cleavage of the alkoxy moiety (cf. **I**, Figure 1a). Luyt and coworkers reported similar hydrogen-bond assisted hydrolysis rate enhancements with aminopropyltrialkoxysilanes.[9] Both the Tacke and Luyt work was primarily motivated by potential applications for polymer end-group reactions. In this study we were interested in enhancing hydrolytic lability of compounds containing relatively stable Si–O–Si motifs (i.e., siloxanes), substructures that have relevance to polymer backbones. More specifically, we have focused on the effect of appending (with various carbon tether lengths) functional groups capable of activating one of the Si–O bonds toward hydrolytic cleavage.

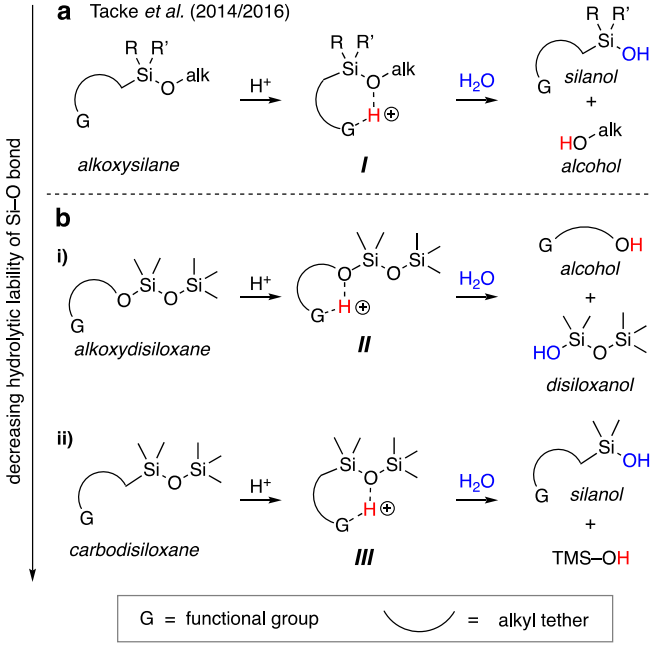

Figure 1. Functional group-assisted hydrolysis of **a**) alkoxysilanes and **b**) i) alkoxydisiloxanes or ii) carbodisiloxanes.

RESULTS AND DISCUSSION

With a longer term interest in degradation of backbone linkages in Si–O-containing polymers, we have studied and report here cleavage reactions of relatively robust siloxane functionalities: namely, alkoxydisiloxanes [RO–Si–O–Si, i) in Figure 1b] and carbodisiloxanes [R–Si–O–Si, ii) in Figure 1b]. Appending tethered functional groups accelerates the hydrolytic cleavage of one of the Si–O bonds in these two types of linkages via internal hydrogen-bond catalysis indicated in species **II** and **III**. To study this phenomenon in greater detail, we prepared and surveyed the hydrolysis behavior of a series of model alkoxydisiloxanes bearing a variety of appended functional groups (e.g., G = methyl ether, methyl ester, ketone, aryl sulfone, phosphine oxide, phosphoramide, etc., some examples of which are shown in Figure 2a). None of these functional groups demonstrated enhanced hydrolysis of either of the two Si–O bonds when compared to the control substrate **1/3-Bu**.

However, substrates having a tethered amide or amine functional group showed significantly pronounced hydrolytic cleavage. To understand the effects of tether length, we systematically varied the length of the alkyl chain (cf. *n* in Figure 2) in series of i) model alkoxydisiloxanes bearing either an appended dimethyl amide (**1**) or a dimethylamino (**3**) functional groups and ii) model carbodisiloxanes bearing the same, appended dimethyl amide (**2**) or a dimethylamino (**4**) functional groups. Before discussing their hydrolysis behavior, we describe next the various syntheses that were used to access the model substrates **1**–**4**.

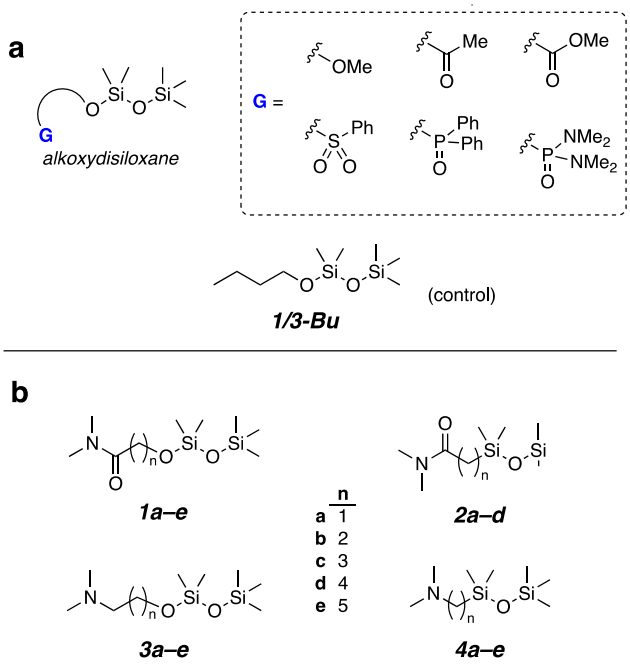

Figure 2. **a)** Model alkoxydisiloxanes that did not demonstrate enhanced hydrolytic behavior relative to the control substrate **1/3-Bu** which lacks a tethered functional group. **b)** Alkoxydisiloxanes (**1** and **3**) and carbodisiloxanes (**2** and **4**) bearing a dimethylamido or dimethylamino functionality appended through tethering alkyl groups of varying lengths.

Preparation of substrates 1–4. The methods used to prepare the alkoxydisiloxanes **1a–e** and **3a–e** (Scheme 1) involved initial synthesis of the dimethylamido- and dimethylamino-alcohols **6** and **7**, respectively, followed by, in each case, their dehydrogenative silylation with pentamethyldisiloxane (**5**). Amido-alcohol **6a** was prepared by ring-opening and amidation of glycolide with dimethylamine. The 3-hydroxypropanamide **6b** was prepared by oxa-Michael addition of benzyl alcohol to dimethylacrylamide.[10] Compounds **6c–e** were accessed by ring-opening butyrolactone, valerolactone, and caprolactone respectively with dimethylamine.

Aminoalcohols **7a–c** were available commercially, and **7d–e** were obtained through LAH reduction of **6d–e**, respectively. We found dehydrogenative silylation[11] of these alcohols with **5** to be a preferable (vs. a chlorosilane alternative) and convenient method for forming the alkoxydisiloxanes to afford **1a–e** and **3a–e**. Following Pd/C catalyst and solvent removal, the dehydrogenative silylation reaction provided product samples that were sufficiently pure for the subsequent hydrolysis studies. Relative to *n*-BuOSi(Me_2)OTMS (**1/3-Bu**), an analog of **1** and **3** having no pendant amide or amine group (G), we observed varying degrees of sensitivity of some of these compounds (e.g., **1a**, **1c**, **3b**, and **3c**) to silica gel chromatography, behavior that subsequently correlated with the rapidity of their Si–O bond cleavage (see later discussion). We did not observe any qualitative differences in the rates of the dehydrogenative silylation reactions of **5** with the alcohols **6a-e** or **7a-e**. The reactions were all quite rapid.

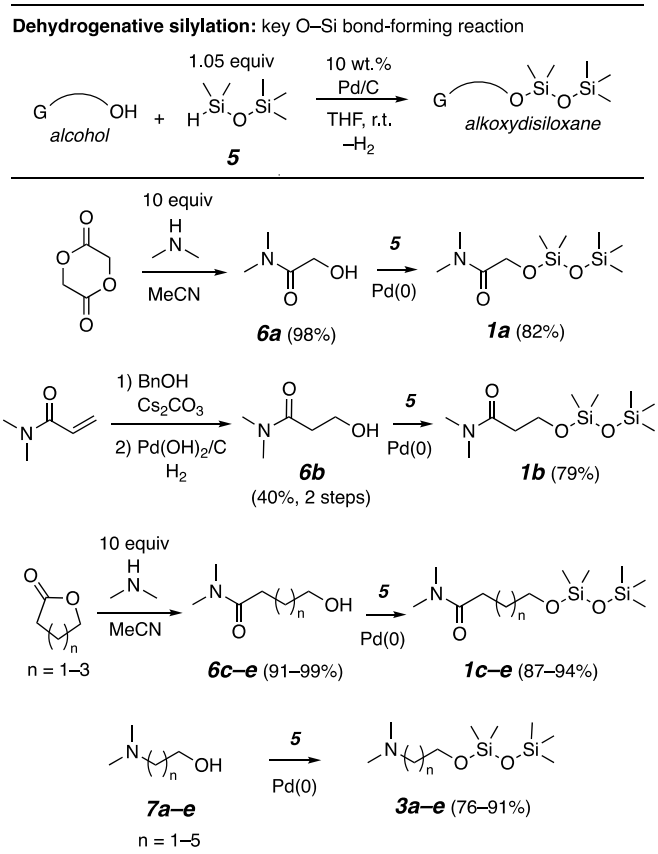

Scheme 1. Synthesis of dimethylamido-alkoxydisiloxanes **1a–e** and dimethylamino-alkoxydisiloxanes **3a–e**.

The syntheses of carbodisiloxanes **2a–d** and **4a-e** required a variety of synthetic approaches (Scheme 2a and 2b, respectively). Compound **2a** was formed through *C*-silylation of the lithium enolate of *N,N*-dimethylacetamide with chlorodisiloxane **8**.[12] The skeleton of **2b** was less straightforward to access; even after screening several catalysts and conditions, direct hydrosilylation of dimethylacrylamide was unsuccessful. However, treating methyl acrylate with the Si–H silane **5** and Wilkinson's catalyst gave a 3:1 mixture of the desired β-hydrosilylation[13] product **9a** and the *trans*-β-silylacrylate **9b**. This mixture was subjected to catalytic hydrogenation, which cleanly converted **9b** to **9a**. The amidation was carried out using trimethylaluminum and dimethylamine, affording **2b**. Exposure of each of the commercially available vinylacetic and 4-pentenoic acids to ~0.01 mol% of Karstedt's catalyst [Pt(0)•divinyltetramethyldisiloxane] and 2.5 equivalents of **5** accomplished both β-hydrosilylation of the alkene and formation of the silyl ester, which, when exposed to a solution of dimethylamine, furnished amidodisiloxanes **2c,d**.

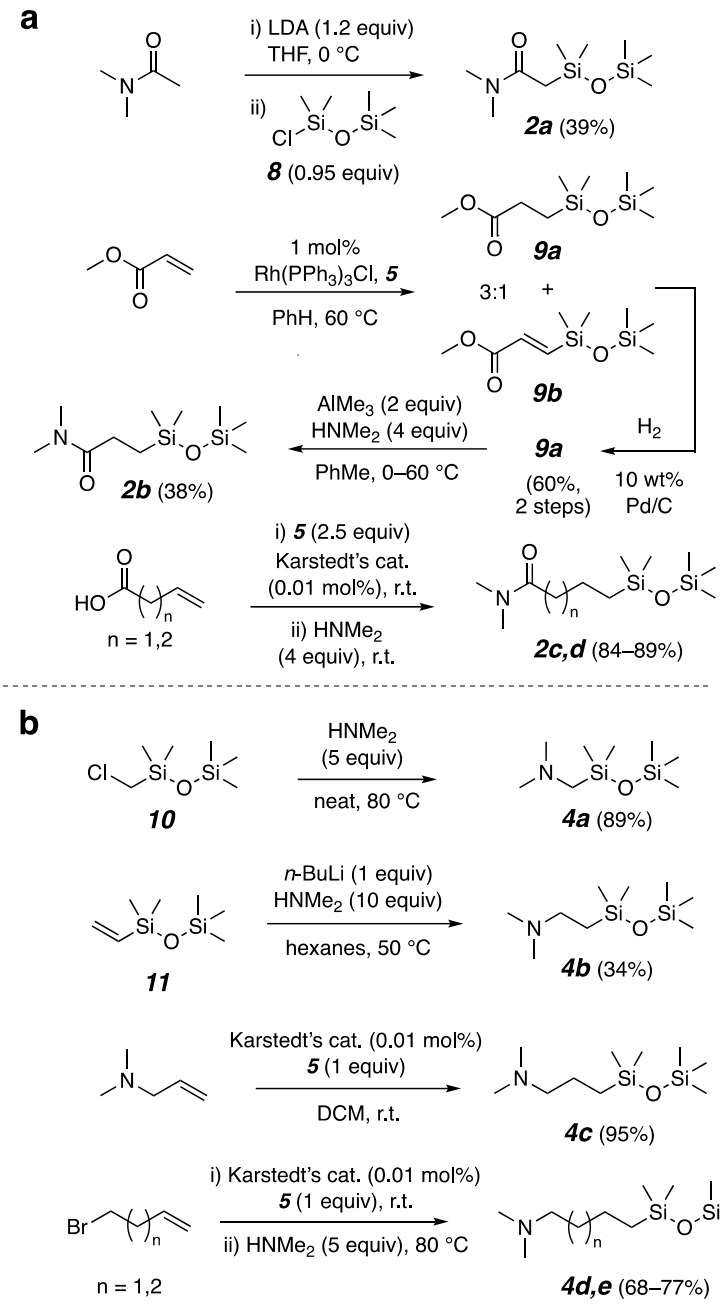

Scheme 2. Synthesis of **a**) dimethylamido-carbodisiloxanes **2a–d** and **b**) dimethylamino-carbodisiloxanes **4a–e**.

Dimethylaminodisiloxane **4a** could be accessed through the S_N2 amination of chloromethyldisiloxane **10** at elevated temperature (Scheme 2b). However, a similar approach

for the preparation of **4b** using the corresponding chloroethyldisiloxane was unsuccessful. As noted by Sommer *et al.,* the direct displacement of β-chlorosilanes with nucleophiles often leads to low yields because of an elimination pathway initiated by nucleophilic attack at silicon accompanied by extrusion of ethylene (cf. TMSE-ester cleavage with fluoride ion).[14] The successful approach involved the addition of $LiNMe_2$ to vinyldisiloxane **11** (in the presence of excess dimethylamine) to afford the β-dimethylaminodisiloxane **4b**.[15] Commercially available dimethylallylamine was a suitable substrate for hydrosilylation with Karstedt's catalyst and **5** to furnish **4c**. In most cases, Karstedt's catalyst selectively (>95%) produced the anti-Markovnikov (linear) product, but we did observe ca. 10% of the branched regioisomer of **4c**. Compounds **4d,e** were accessed by the hydrosilylation of 4-bromo-1-butene and 5-bromo-1-pentene with Karstedt's catalyst and **5**, followed by S_N2 reaction with excess dimethylamine. The hydrosilylation reactions between **5** and the alkenes in Scheme 2 occurred with different rates, but this was likely more a function of the electronic nature of the substituent directly on the alkene rather than of an effect induced by the more remote functional group.

Hydrolysis of alkoxydisiloxanes 1a–e (amides) and 3a–e (amines). The relative rates of hydrolysis of **1a–e** and **3a–e** were studied *in situ* by ^{1}H NMR spectroscopy (Figure 3a). A small sample of each compound (0.025 mmol, between 5–12 mg) was dissolved in 0.45 mL of MeCN-d_3 and an initial spectrum of the substrate recorded. A stock solution of D_2O and AcOD-d_3 (40 μL, 4:1 vol/vol) was then added and spectra were collected at varying intervals, depending on the hydrolytic lability of each substrate. Samples were analyzed in triplicate. The rates of hydrolysis were measured over the course of 10 minutes to several hours. Because all of these

reactions were free from any significant byproducts and proceeded to completion, the $t_{1/2}$ of the reactions (i.e., the time required for the relative amounts of starting material and product to be equal) could be directly measured by integrating well-resolved diagnostic resonance(s) in the starting alkoxydisiloxane vs. that of the resulting free alcohol product (Figure 3b). A typical set of spectral data is shown in Figure 3b. The chemical shifts of the methylene CH_2O protons in the alkoxy moiety were well-resolved, and their relative intensities reflect the rate of hydrolysis. A sample set of ^{1}H NMR data for the hydrolysis of **1c** are shown in Figure S1 (see Supporting Information).

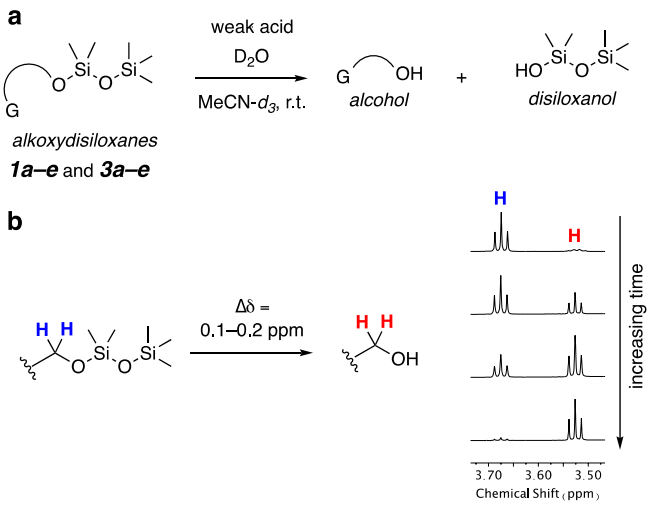

Figure 3. **a**) Hydrolysis reactions of alkoxydisiloxanes **1a–e** and **3a–e**. **b**) Example of the changes observed by ^{1}H NMR monitoring of an alkoxydisiloxane.

The relative rates of the hydrolysis of dimethylamido-alkoxydisiloxanes **1a**–**e** are shown in Figure 4a. The products were pentamethydisiloxanol and the corresponding amidoalcohol (Figure 3a); there was no evidence in the NMR (or GC-MS) data to suggest that cleavage at the

Si–O–Si linkage, which would have generated ROSi(Me)2OH and TMSOH, had occurred. As a control experiment, we also subjected the *n*-butyl alkoxydisiloxane **1/3-Bu**, which has no tethered functional group, to the same hydrolysis conditions. To check whether the faster hydrolysis rates of **1a–e** were the results of intramolecular activation and not an intermolecular interaction with other amide functional groups, we doped in a large quantity (50 µL) of *N,N*-dimethylacetamide (DMAc) to the reaction mixture containing **1/3-Bu**. This modification did not appreciably affect the rate of hydrolysis, which supports our interpretation of intramolecular activation.

All of **1a**–**e** were cleaved faster than **1/3-Bu** with the largest rate enhancement shown by **1a** (ca. 50x). Our working mechanistic hypothesis was that the protonated amide **II** (Figure 4b) was an essential intermediate for activation of the alkoxy oxygen atom through the indicated intramolecular hydrogen bond. With one notable exception, the relative rates of cleavage decreased within the series **1a**–**e** with increasing ring size of the hydrogen-bonded species. The outlier substrate was **1b**, which reacted only 2x faster than the unactivated control substrate **1/3-Bu** and 25x slower than **1a**. This was surprising because **1b** would involve a seemingly reasonable six-atom array in the hydrogen bonded species **II**. Did this mean that the mechanistic thinking was misguided or was some other non-obvious factor in play?

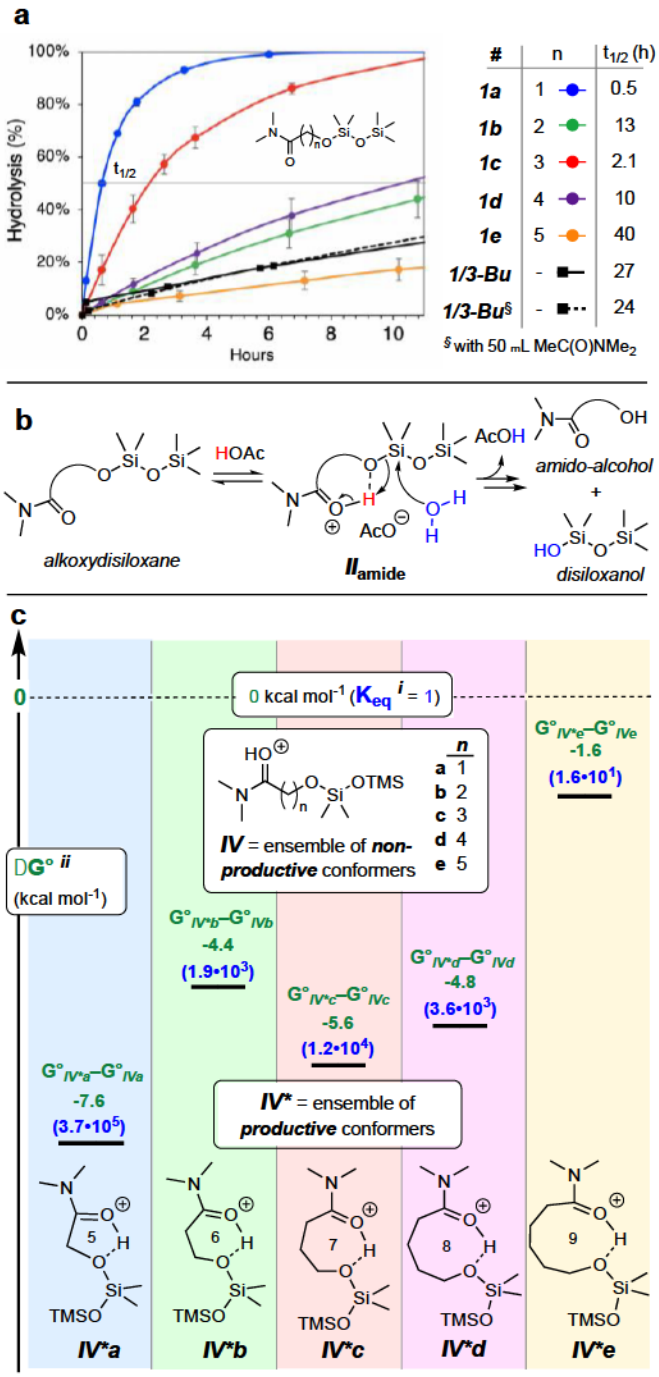

Figure 4. **a**) Hydrolysis rates for amide substrates **1a–e**. **b**) Depiction of hydrolysis involving assistance by the endocyclic hydrogen bond in $\mathbf{II}_{\mathbf{amide}}$. **c**) DFT-computed ΔG°s (green) (and the associated K_{eq}s (blue)) of the ensembles comprised of productive (**IV***) vs. non-productive (**IV**)

conformers for each of the species corresponding to protonated forms of **1a–e**, which differ by the length of their alkyl tethers. [SMD(acetonitrile)/M06-L/6-31G(d)].

[i] $K_{eq} = \frac{\sum \chi_{IV^*}}{\sum \chi_{IV}}$, where χ is the Boltzmann-weighted mole fraction of each conformer.

[ii] $\Delta G^{\circ} = -\mathrm{RT}\ln(K_{eq})$, where *R* is the gas constant and *T* is 298 K.

To identify factor(s) that could account for the observed rates of hydrolysis of the amides **1a–e**, we undertook a density functional theory (DFT) computational analysis (Figure 4c). The choice of functional and basis set was made based on a study that assessed the accuracy of a variety of DFT methods at predicting proton affinity and condensation enthalpy for various silanes/siloxanes in the gas phase and in water.[16] A full molecular mechanics conformational search was performed on each of the five amide substrates **IVa–e**. Each conformer was optimized by DFT. The conformers for each substrate **a-e** were then binned as either productive (**IV***) or non-productive (**IV**); if the proton showed a H-bond to the proximal siloxane oxygen atom having a distance of less than 3.2 Å, the structure was deemed productive. Otherwise, the conformer was considered unproductive. the proton did not show H-bonding to either siloxane oxygen atom, the conformer was considered non-productive. The sum of the Boltzmann-weighted energies of the ensemble of all productive conformers vs. that of all non-productive conformers, for a given tether length, resulted in a ΔG° value, which was then converted to a K_{eq}. These are the data graphed in Figure 4c.

Notably, the relative populations of these productive (*i.e.* reactive) conformations and the observed rates of hydrolysis of **1a–e** were reasonably well correlated, including for the outlier substrate **1b**. Together, we take these results as support that the cyclic species $\mathbf{II_{amide}}$ is the key reactive intermediate on the reaction coordinate.

Although dialkylamides are among the most basic of the carbonyl-containing functional groups,[17] amines are considerably more basic. It stood to reason, then, that alkoxydisiloxane substrates bearing tethered dimethylamino groups (**3a–e)** might hydrolyze more quickly than their dimethylamide analogs. If a protonated and internally hydrogen bonded species was indeed the key intermediate responsible for the enhanced hydrolysis, the concentration of that reactive species for **3a–e** would be considerably higher than for the analogous amides (Figure 5b). The central role of functional group basicity is further supported by the fact that the classes of compounds shown in Figure 1a, all less basic than alkyl amides, did not demonstrate enhanced hydrolysis behavior when compared to **1/3-Bu**. Under the same conditions used for the amide studies (i.e., 0.45 mL of MeCN-d_3, 8 μL of CD_3CO_2D, 32 μL of D_2O) **3b–c** hydrolyzed so rapidly that the hydrolysis reaction was complete even at the earliest time point. To slow the rate, we changed to using phenol, a much weaker Brønsted acid catalyst (0.5 mL of MeCN-d_3, 20 mg of phenol, 20 μL of D_2O). Under these conditions, **3b–c** had $t_{1/2}$s of ca. 6 and 5 hours, respectively, but **3a** and **3d–e** did not hydrolyze to an extent greater than 5% over the course of 12 hours (solid lines in graph, Figure 5a). We then went back and exposed **3a** and **3d–e** to the AcOD-d_3 conditions (dashed lines in graph, Figure 5a). We observed rapid hydrolysis of **3a** ($t_{1/2}$= 15 min), but much slower for **3d–e**, suggesting enthalpic (torsional/transannular strain) destabilization of the cyclic hydrogen bonded intermediates $\mathbf{II_{amine}}$ having 8- and 9-membered rings (Figure 5b). Nonetheless, all amine-bearing substrates hydrolyzed at least somewhat more quickly than **1/3-Bu** (cf. Figure 4a), demonstrating the utility of the basic functional group assistance even at large ring sizes (cf. **3d–e**).

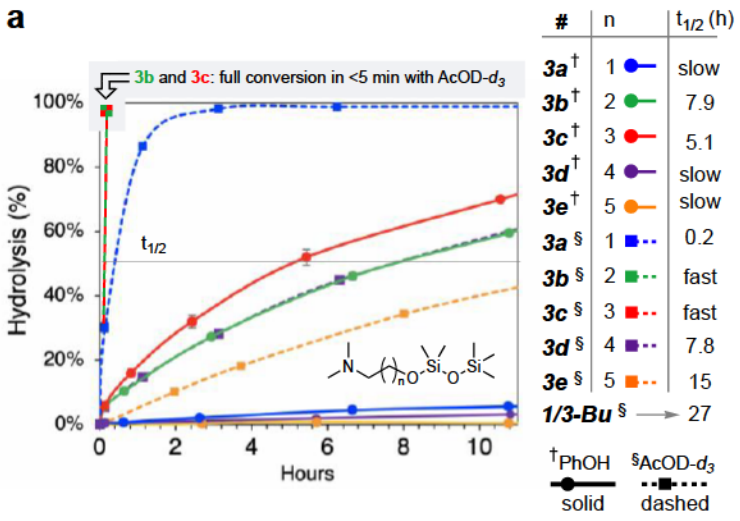
a
3b and 3c: full conversion in <5 min with AcOD-d_3
Hydrolysis (%)
100%
80%
60%
40%
20%
0%
$t_{1/2}$
0
2
4
6
8
10
Hours
| n | $t_{1/2}$ (h)
3a † 1 slow
3b † 2 7.9
3c † 3 5.1
3d † 4 slow
3e † 5 slow
3a § 1 0.2
3b § 2 fast
3c § 3 fast
3d § 4 7.8
3e § 5 15
1/3-Bu § 27
†PhOH solid
§AcOD-d_3 dashed

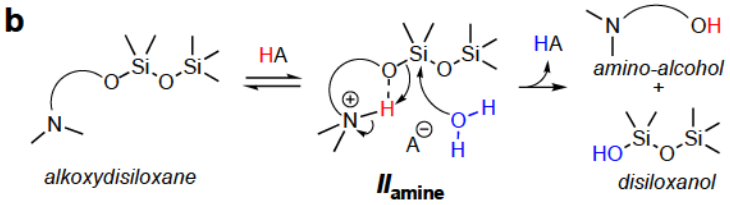
b
HA
HA
alkoxydisiloxane
II_{amine}
amino-alcohol
+
disiloxanol

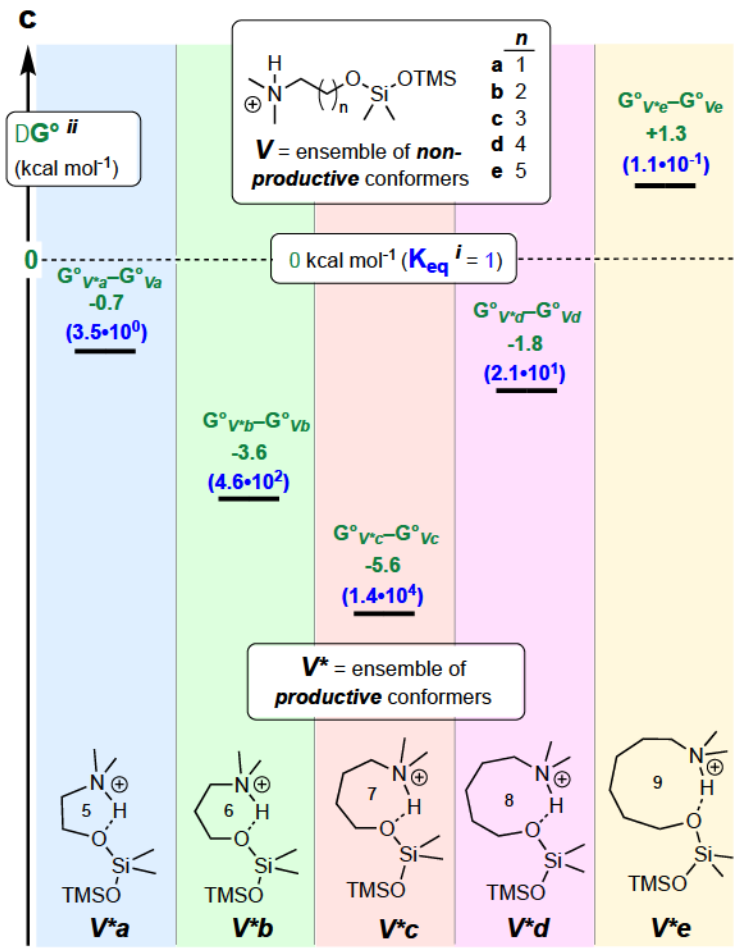
c
DG° ii (kcal mol-1)
n
a 1
b 2
c 3
d 4
e 5
V = ensemble of non-productive conformers
0
0 kcal mol-1 (K_{eq} i = 1)
G°V*a–G°Va -0.7 (3.5•10^0)
G°V*b–G°Vb -3.6 (4.6•10^2)
G°V*c–G°Vc -5.6 (1.4•10^4)
G°V*d–G°Vd -1.8 (2.1•10^1)
G°V*e–G°Ve +1.3 (1.1•10^-1)
V* = ensemble of productive conformers
TMSO
V*a
V*b
V*c
V*d
V*e

Figure 5. **a**) Hydrolysis data for amine substrates **3a–e** using either phenol (solid lines with circles) or AcOD (dashed lines with squares) as the Bronsted acid catalyst. **b**) Depiction of hydrolysis involving assistance by the endocyclic hydrogen bond in **II-amine**. **c**) DFT-computed ΔG°s (green) (and the associated K_{eq}s (blue)) of the ensembles comprised of productive (**V***) vs. non-productive (**V**) conformers for each of the species corresponding to protonated forms of **3a–e**, which differ by the length of their alkyl tethers. [SMD(acetonitrile)/M06-L/6-31G(d)].

[i] $K_{eq} = \frac{\sum \chi_{V^*}}{\sum \chi_V}$, where χ is the Boltzmann-weighted mole fraction of each conformer.

[ii] $\Delta G^\circ = -\mathrm{RT}\ln(K_{eq})$, where *R* is the gas constant and *T* is 298 K.

We performed an analogous set of DFT calculations on the amines **3a–e** (Figure 5c) as those conducted for amides **1a–e** to learn whether they would show a similar correlation between the relative hydrolysis rates of **3a–e** and the calculated ΔG°s (the difference between the Boltzmann-averaged energies of all productive conformers for a given tether length (e.g., **V*a)** and the non-productive conformers (e.g., **Va**). The amine computations correlated well with the observed hydrolysis data for **3a–e**. For example, species **V*c/Vc** showed the largest population of productive conformers and had the fastest rate of hydrolysis (Figure 5a); conversely, species **V*e/Ve** were computed to have the lowest population of productive conformers (ca. 10%) and had the slowest rate of hydrolysis.

To summarize the observations with the series of alkoxydisiloxanes, we measured the relative rates of hydrolysis of those containing amido or amino functional groups connected by alkyl tethers of various lengths. The involvement of key hydrogen-bonded, cyclic intermediates

II$_{amide}$ or **II**$_{amine}$ are proposed and supported by DFT computation of the energy difference between the productive (**IV*** and **V***) and non-productive (**IV** and **V**) conformers. The trends observed in the relative rates of cleavage correlate well with the computational results.

Cleavage reactions of carbodisiloxanes 2a–d (amides) and 4a–e (amines). The hydrolysis behavior of the carbodisiloxanes was seen to be similar to that of the alkoxydisiloxanes. For example, when the amide **2b** was treated under the standard hydrolysis conditions and monitored by ^{1}H NMR spectroscopy, formation of the silanols **12** and **13** was observed. However, in contrast to the alkoxydisiloxanes, the reaction did not proceed to completion. Instead, an equilibrium mixture of the starting material **2b**, the hydrolysis products **12** and **13**, as well as the symmetrical disiloxane **14** was formed (Figure 6a). Interestingly, trimethylsilanol (**13**) did not dehydrate to form hexamethyldisiloxane (**15**) under these reaction conditions. The relative equilibrium amounts of **2b** and **12**–**14** varied with the concentration of water in the NMR sample. The amine **4b** showed similar behavior (Figure 6b), producing an equilibrium mixture of **4b**, silanols **16** and **13**, and the symmetrical disiloxane **17**. Unsurprisingly, we observed no hydrolysis after several weeks of a carbodisiloxane bearing no tethered functional group (cf. **20**, Figure 7b). A sample set of ^{1}H NMR data for the hydrolysis of **4b** is shown in Figure S2 (see Supporting Information).

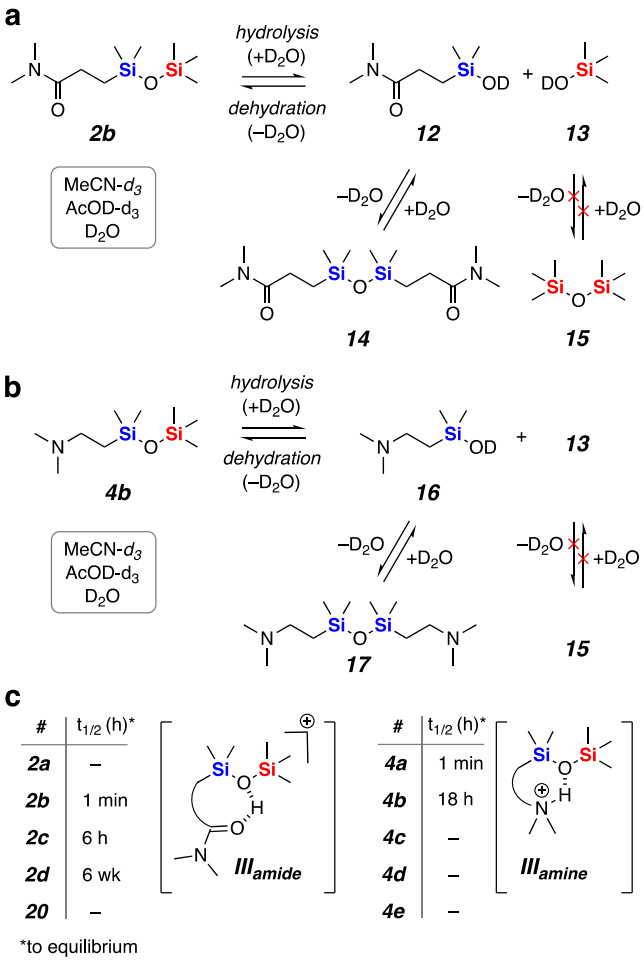

Figure 6. **a)** Representative hydrolysis and dimerization equilibria of the amido carbodisiloxane **2b** to form the silanols **12** and **13** and the symmetrical disiloxane **14**. **b)** Representative hydrolysis and dimerization equilibria of the amino carbodisiloxane **4b** to produce the silanols **16** and **13** and the symmetrical disiloxane **17**. **c)** Approximate half-lives to reach equilibrium via the presumed hydrogen-bonded intermediates $\mathbf{III_{amide}}$ and $\mathbf{III_{amine}}$ for hydrolysis of **2b–d** and **4a–b**.

Qualitatively, compared to the alkoxydisiloxanes, we observed a much wider variation of relative rates (see data in Figure 6c) among the dimethylamido-carbodisiloxanes **2b–d**. Here, we use $t_{1/2}$ to mean half the time required to reach the equilibrium ratio of products. While **2b** equilibrated in minutes, the longer homolog **2c** required approximately 12 hours to equilibrate, and **2d** took weeks to show any significant change. Similarly, the dimethylamino-carbodisiloxane **4a** equilibrated rapidly (minutes), while the longer homologs **4c–e** did not show any signs of hydrolysis after several weeks. These observed differences in relative rates of hydrolysis are consistent with a picture in which species such as $\mathbf{III}_{\mathbf{amide}}$ and $\mathbf{III}_{\mathbf{amine}}$ are relevant intermediates responsible for activation of the Si–O cleavage.

In the early phase of observing the experiments like those described in Figure 6, we considered the possibility of a silanol reacting directly with a disiloxane in a siloxy-metathesis reaction. To probe this possibility, we carried out experiments like the ones shown in Figure 7a. Exposing **4a** to one equivalent of triethylsilanol (**18**) in acetonitrile at ambient temperature resulted in exchange between the trimethyl- and triethylsilyloxy moieties and quickly (< 2 h) came to rest at an ca. 1:1 equilibrium ratio between **4a**/**18** and **19a**/**13** (GC-MS analysis). Notably, no acid was required to promote this facile exchange reaction. A similar outcome was seen, albeit more slowly, using the amine **4b**. None of **4c–e** or the amides **2a–e** underwent this rapid siloxy exchange under these conditions. The enabling role of the pendant amine was demonstrated by the control experiment shown in Figure 7b. No appreciable exchange (or scrambling) was seen between the disiloxane **20** and silanol **18**.

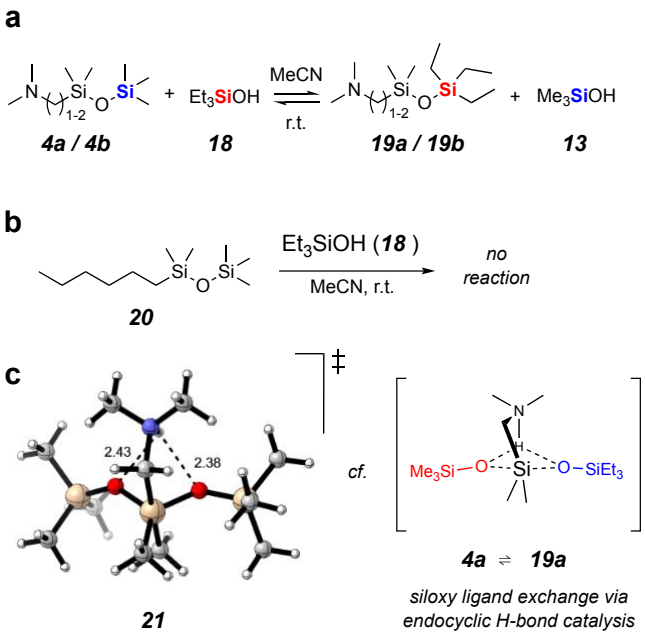

Figure 7. Siloxy ligand exchange. **a**) Facile equilibration of **4a/b** with **18a/b** under neutral conditions. **b**) A negative control experiment demonstrating an activation role of the pendant amine groups on **4a/b**. **c**) A transition structure located on the reaction coordinate identified by DFT computation modeling the ligand exchange within **4a**. [SMD(acetonitrile)/M06-L/6-31+G(d,p)]

We probed this interesting exchange process computationally (Figure 7c). Using the simplified, degenerate, model exchange reaction between amine **4a** and trimethylsilanol (**13**), we identified the transition structure **21**, arising from the 1:1 hydrogen-bonded complex between **4a** and the neutral silanol **13**, in which the pendant amine shuttled the proton between the oxygen atoms of the entering and departing R_3Si–O moieties (cf. **4a** ⇌ **19a**) The activation barrier was merely 4.2 kcal mol^{-1}.

Finally, the cleavage behavior of the amide **2a** was unique from any others (Figure 8). Hydrolysis to liberate *N,N*-dimethylacetamide (**22**) and the disiloxanol **23** was observed in

acetonitrile in the absence of any added acid. Similarly, silanolysis (with **18**) produced **22** along with the trisiloxane **24**. Each of these Si–C cleavage processes can be rationalized by six-membered ring structures such as **25a/b** in which the protic OH is coordinated to the amide carbonyl oxygen atom to promote addition of the water or silanol oxygen atom, respectively, to the proximal silicon atom.

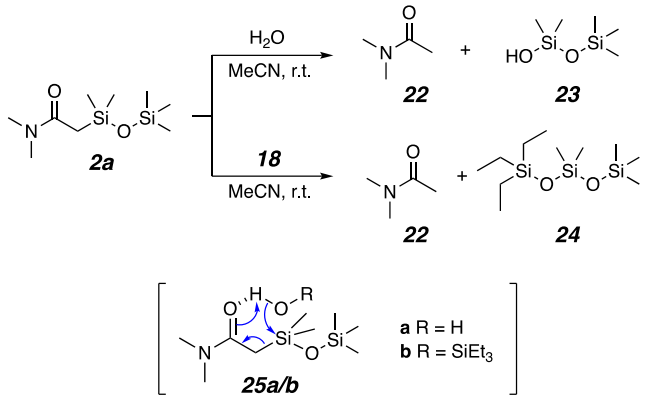

Figure 8. Si–C bond cleavage of amido-disiloxane **2a** by hydrolysis or silanolysis.

Several additional general observations about the hydrolysis reactions described here are worth mentioning. One might wonder if the silanol species released during the cleavage of **1** or **3** might further catalyze the reaction. Silanols are weaker acids than acetic acid and the latter was used in molar excess over that of the siloxane substrates. Monitoring of reactions over the time course of the hydrolysis, which was routinely done to deduce the half-lives, showed no evidence of any significant amount of autocatalysis by the silanol products of the hydrolyses.

CONCLUSION

In conclusion, we have measured the relative rates of hydrolysis of alkoxydisiloxanes featuring amido or amino functional groups connected by alkyl tethers of various lengths. The

involvement of key hydrogen-bonded cyclic intermediates $\mathbf{II}_{\mathbf{amide}}$ or $\mathbf{II}_{\mathbf{amine}}$ are supported by DFT computation of the relative populations of the productive vs. the non-productive conformers. The trends observed in the relative rates of hydrolysis correlate well with the computational results. We have also studied the hydrolysis behavior of carbodisiloxanes bearing pendant amido or amino functional groups. Rather than the essentially complete hydrolysis observed for the alkoxydisiloxanes, the carbodisiloxanes came to rest at an equilibrium mixture of the starting material, hydrolyzed silanols, and symmetrical bis-amido or bis-amino disiloxane. The relative rates of the carbodisiloxane hydrolyses spanned a wider range than for the alkoxydisiloxanes. An interesting siloxy exchange reaction between an external silanol and the carbodisiloxane bearing a pendant amine was discovered. The understanding gained through these studies enables future investigation of substrates having more complex, Si–O-containing substructures (e.g., cf. the trisiloxane **24**). Moreover, given our longer-term interest in silicone polymer backbone degradation, we envision that these results can guide the incorporation of pendant groups to enable controlled degradation of Si–O-containing polymer backbones.

DATA AVAILABILITY STATEMENT

- The principal data underlying this study are available in the online supporting information (SI), as delineated below.

SUPPORTING INFORMATION

- Experimental details for preparation of and characterization data for all new compounds and representative hydrolysis ^{1}H NMR data, and discussion of computational methods (PDF).
- "Appendix of Computational Data" containing the cartesian coordinates and Gibbs energies for all computed structures (PDF).
- "FID for Publication": FAIR NMR data, comprising the primary ^{1}H and ^{13}C NMR (and select ^{29}Si) FID files for compounds **1a**, **1b**, **1c**, **1c-hydrolysis**, **1d**, **1e**, **2a**, **2b**, **2c**, **2d**, **3a**, **3b**, **3c**, **3d**, **3e**, **4a**, **4b**, **4b-hydrolysis**, **4c**, **4d**, **4e**, **9a**, **14**, **17**, and **1/3-Bu** and a master metadata Word file (ZIP folder).

AUTHOR INFORMATION

Corresponding Authors:

Thomas R. Hoye Department of Chemistry, University of Minnesota, 207 Pleasant Street, SE, Minneapolis, Minnesota 55455, United States; ORCID https://orcid.org/0000-0001-9318-1477; Email: hoye@umn.edu

Theresa M. Reineke Department of Chemistry, University of Minnesota, 207 Pleasant Street, SE, Minneapolis, Minnesota 55455, United States; ORCID https://orcid.org/0000-0001-7020-3450; Email: treineke@umn.edu

Authors:

Ethan A. Gormong Department of Chemistry, University of Minnesota, 207 Pleasant Street, SE, Minneapolis, Minnesota 55455, United States; ORCID https://orcid.org/0000-0002-6568-2458

Dorian S. Sneddon Department of Chemistry, University of Minnesota, 207 Pleasant Street, SE, Minneapolis, Minnesota 55455, United States; ORCID https://orcid.org/0000-0002-7326-1565

Authors Contributions:

E.A.G. performed all the experimental work; D.S.S. performed all the computational work. E.A.G., D.S.S., T.M.R., and T.R.H. interpreted the data and cowrote the manuscript.

Notes:

The authors declare no competing financial interest.

ACKNOWLEDGEMENTS

This research was supported by the National Science Foundation Center for Sustainable Polymers (CHE-1901635), an NSF-funded Center for Chemical Innovation (CCI). Support for NMR instrumentation came from a Shared Instrumentation Grant (NIH S10OD011952). Mass spectrometry data were collected using instrumentation from The University of Minnesota Department of Chemistry Mass Spectrometry Laboratory (MSL), supported in part by The National Science Foundation (NSF, Award CHE-1336940). DFT calculations were carried out using resources provided at the Minnesota Supercomputing Institute. D.S.S. appreciates the support from a Wayland E. Noland Fellowship.

REFERENCES

(1) Eguchi, T.; Sudo, A.; Endo, T. Polycondensation of Trialkoxysilane Monomers Accelerated by Neighboring Group Participation of Urea Moiety. *J. Polym. Sci. Part Polym. Chem.* **2008**, *46*, 6654–6659.

(2) Nishimura, Y.; Chung, J.; Muradyan, H.; Guan, Z. Silyl Ether as a Robust and Thermally Stable Dynamic Covalent Motif for Malleable Polymer Design. *J. Am. Chem. Soc.* **2017**, *139*, 14881–14884.

(3) Wohl, A. R.; Michel, A. R.; Kalscheuer, S.; Macosko, C. W.; Panyam, J.; Hoye, T. R. Silicate Esters of Paclitaxel and Docetaxel: Synthesis, Hydrophobicity, Hydrolytic Stability, Cytotoxicity, and Prodrug Potential. *J. Med. Chem.* **2014**, *57*, 2368–2379.

(4) Zhang, S.; Xu, X.-Q.; Liao, S.; Pan, Q.; Ma, X.; Wang, Y. Controllable Degradation of Polyurethane Thermosets with Silaketal Linkages in Response to Weak Acid. *ACS Macro Lett.* **2022**, *11*, 868–874.

(5) Hwu, R. J.-R.; Tsay, S.-C.; Cheng, B.-L. Steric Effects of Silyl Groups. In *The Chemistry of Organic Silicon Compounds*; John Wiley & Sons, Ltd, 1998; pp 431–494.

(6) (a) Gölitz, H. D.; Degener, E.; Oertel, G.; Simmler, W.; Schmelzer, H.-G. (Farbenfabriken Bayer AG) DE 1812562; June 18, 1970. (b) Gölitz, H.-D.; Simmler, W. (Farbenfabriken Bayer AG) DE 1812564; June 18, 1970. (c) Gölitz, H. D.; Schwabe, P.; Simmler, W. (Farbenfabriken Bayer AG) DE 1694209; April 8, 1971. (d) Wagner, K.; Oertel, G.; Gölitz, H. D.; Quiring, B. (Bayer AG) DE 2155260; May 10, 1973. (e) Thom, K.-F.; Sattlegger, H.; Wagner, K. (Bayer

AG) DE 2445220; April 8, 1976. (f) Thom, K.-F.; de Montigny, A. (Bayer AG) DE 2500020; July 15, 1976. (g) Thom, K.-F.; Goller, H. (Bayer AG) DE 2543966; April 7, 1977.

(7) Berkefeld, A.; Guerra, C. F.; Bertermann, R.; Troegel, D.; Daiß, J. O.; Stohrer, J.; Bickelhaupt, F. M.; Tacke, R. Silicon α-Effect: A Systematic Experimental and Computational Study of the Hydrolysis of Cα- and Cγ-Functionalized Alkoxytriorganylsilanes of the Formula Type $ROSiMe_2(CH_2)NX$ (R = Me, Et; n = 1, 3; X = Functional Group). *Organometallics* **2014**, *33*, 2721–2737.

(8) Ehbets, J.; Lorenzen, S.; Mahler, C.; Bertermann, R.; Berkefeld, A.; Poater, J.; Fritz-Langhals, E.; Weidner, R.; Bickelhaupt, F. M.; Tacke, R. Synthesis and Hydrolysis of Alkoxy(Aminoalkyl)Diorganylsilanes of the Formula Type $R_2(RO)Si(CH_2)NNH_2$ (R = Alkyl, n = 1–3): A Systematic Experimental and Computational Study. *Eur. J. Inorg. Chem.* **2016**, *11*, 1641–1659.

(9) Issa, A. A.; El-Azazy, M.; Luyt, A. S. Kinetics of Alkoxysilanes Hydrolysis: An Empirical Approach. *Sci. Rep.* **2019**, *9*, Art. No. 17624.

(10) Yamada, T.; Okaniwa, N.; Saneyoshi, H.; Ohkubo, A.; Seio, K.; Nagata, T.; Aoki, Y.; Takeda, S.; Sekine, M. Synthesis of 2'-O-[2-(N-Methylcarbamoyl)Ethyl]Ribonucleosides Using Oxa-Michael Reaction and Chemical and Biological Properties of Oligonucleotide Derivatives Incorporating These Modified Ribonucleosides. *J. Org. Chem.* **2011**, *76*, 3042–3053.

(11) Scott, C. N.; Wilcox, C. S. A Mild Synthesis of Unsymmetrical Bis-Alkoxysilanes through Catalyzed Alcoholysis of Hydridosilanes. *Synthesis* **2004**, *14*, 2273–2276.

(12) Woodbury, R. P.; Rathke, M. W. Reaction of Lithium N,N-Dialkylamide Enolates with Trialkylchlorosilanes. *J. Org. Chem.* **1978**, *43*, 881–884.

(13) Ojima, I.; Kumagai, M.; Nagai, Y. Hydrosilylation of α,β-Unsaturated Nitriles and Esters Catalyzed by Tris (Triphenylphosphine)Chlororhodium. *J. Organomet. Chem.* **1976**, *111*, 43–60.

(14) Sommer, L. H.; Bailey, D. L.; Goldberg, G. M.; Buck, C. E.; Bye, T. S.; Evans, F. J.; Whitmore, F. C. Vinylsilanes, Chlorovinylsilanes and β-Styryltrimethylsilane. Further Studies on the Silicon α-Effect and β-Eliminations Involving Silicon. *J. Am. Chem. Soc.* **1954**, *76*, 1613–1618.

(15) Nagasaki, Y.; Morishita, S.; Kato, M.; Kihara, Y.; Tsuruta, T. Reactivity of Lithium Alkylamide toward Vinylsilane Derivatives. *Bull. Chem. Soc. Jpn.* **1992**, *65*, 949–953.

(16) Cypryk, M.; Gostyński, B. Computational Benchmark for Calculation of Silane and Siloxane Thermochemistry. *J. Mol. Model.* **2016**, *22*, Art. No. 35.

(17) Bagno, A.; Scorrano, G. Acid-Base Properties of Organic Solvents. *J. Am. Chem. Soc.* **1988**, *110*, 4577–4582.